

*Original Research*

# Involvement of CXCL10 in Neuronal Damage under the Condition of Spinal Cord Injury and the Potential Therapeutic Effect of Nrg1

Xin-yu Qiao<sup>1</sup>, Yi Wang<sup>1</sup>, Wei Zhang<sup>1,2</sup>, Qian Li<sup>1</sup>, Chong Liu<sup>1</sup>, Ji-ji Dao<sup>1</sup>, Chen-meng Qiao<sup>3</sup>, Chun Cui<sup>3</sup>, Yan-qin Shen<sup>3</sup>, Wei-jiang Zhao<sup>1,\*</sup>

<sup>1</sup>Cell Biology Department, Wuxi School of Medicine, Jiangnan University, 214122 Wuxi, Jiangsu, China

<sup>2</sup>Department of Pathogen Biology, Guizhou Nursing Vocational College, 550081 Guiyang, Guizhou, China

<sup>3</sup>Department of Neurodegeneration and Neuroinjury, Wuxi School of Medicine, Jiangnan University, 214122 Wuxi, Jiangsu, China

\*Correspondence: [weijiangzhao@jiangnan.edu.cn](mailto:weijiangzhao@jiangnan.edu.cn) (Wei-jiang Zhao)

Academic Editor: Gernot Riedel

Submitted: 26 December 2022 Revised: 8 February 2023 Accepted: 13 February 2023 Published: 13 July 2023

## Abstract

**Objective:** Few studies have reported the direct effect of C–X–C motif chemokine ligand 10 (CXCL10) and Neuregulin 1 (Nrg1) on neurons after spinal cord injury (SCI). This study reports the role of CXCL10 in the regulation of neuronal damage after SCI and the potential therapeutic effect of Nrg1. **Methods:** The expression level of *CXCL10* and *Nrg1* in SCI mice was analyzed in the Gene Expression Omnibus DataSets, followed by immunohistochemical confirmation using a mouse SCI model. HT22 cells and NSC34 cells were treated with CXCL10 and Nrg1, individually or in combination, and then assayed for cell viability. The percentage of wound closure was determined through the cell scratch injury model using HT22 and NSC34 cells. Potential molecular mechanisms were also tested in response to either the individual administration of CXCL10 and Nrg1 or a mixture of both molecules. **Results:** *CXCL10* expression was significantly increased in both young and old mice subjected to SCI, while *Nrg1* expression was significantly decreased. CXCL10 induced a decrease in cell viability, which was partially reversed by Nrg1. CXCL10 failed to inhibit scratch healing in HT22 and NSC34 cells, while Nrg1 promoted scratch healing. At the molecular level, CXCL10-activated cleaved caspase 9 and cleaved caspase 3 were both inhibited by Nrg1 through pERK1/2 signaling in HT22 and NSC34 cells. **Conclusions:** CXCL10 is upregulated in SCI. Despite the negative effect on cell viability, CXCL10 failed to inhibit the scratch healing of HT22 and NSC34 cells. Nrg1 may protect neurons by partially antagonizing the effect of CXCL10.

**Keywords:** spinal cord injury (SCI); HT22 cells; NSC34 cells; C–X–C motif chemokine ligand 10 (CXCL10); Neuregulin 1 (Nrg1); neuronal damage; cell viability; scratch injury

## 1. Introduction

Spinal cord injury (SCI) causes a series of complex pathological changes, such as neuronal damage, cell death as well as inflammation, and also leads to complex secondary injuries [1]. Studies have shown that many molecules in the microenvironment may play a role in the pathological progression of SCI [2]. Certain molecules like C–X–C motif chemokine ligand 10 (CXCL10) and Neuregulin 1 (Nrg1) are related to the process of SCI [3–6]. Thus, they may act as potential therapeutic targets in this process [7].

Currently, some studies have shown that CXCL10 is up-regulated after SCI. In the spinal cord of rats with SCI, the expression level of CXCL10 is significantly higher at 12 hours post-injury and is attenuated to the same level as that for the control group at 24 hours post-injury [8]. In a mouse model of SCI, CXCL10 mRNA is highly expressed in the spinal cord 30 minutes post-injury [9]. In patients with SCI, the serum level of CXCL10 reaches a peak at day seven. Such observations contribute to the identification of CXCL10-targeted therapy after SCI. A recent finding confirms that CXCL10 neutralization reduces inflam-

mation and neuronal damage [10]. A further novel finding demonstrated that CXCL10 triggers apoptosis in fetal neurons [11]. According to the foregoing research, it was speculated by the authors that CXCL10 may induce neuronal death via its apoptosis-promoting effect after SCI.

Nrg1 acts as an endogenous repair-modulating molecule in the central nervous system [12]. However, the role of Nrg1 in regeneration repair is primarily focused on axon remyelination and the response of microglia and astrocytes regulated by Nrg1 [13–15]. Few studies have focused on the direct effect of Nrg1 signaling on neurons *in vivo* after SCI. In heme-induced cortical organoid injury, Harbuzariu *et al.* [16] revealed that Nrg1 significantly reduced the expression of CXCL10-receptor CXCR3 and attenuated ongoing apoptosis and structural changes in neurons. It is thus hypothesized here that Nrg1 may exert neuronal protection by antagonizing the pathological effect of CXCL10.

In this study, the expression levels of CXCL10 and Nrg1 in SCI mice were documented by bioinformatic analysis and animal experiments. CXCL10 was highly expressed, while Nrg1 was reduced after SCI. CXCL10 did



not inhibit wound closure in either HT22 or NSC34 cells. The neuroprotective effect and the potential molecular mechanisms of Nrg1 against CXCL10 were tested in both HT22 and NSC34 cells. This study extends understanding of the role of CXCL10 and Nrg1 in SCI, indicating that they may act as potential therapeutic targets in SCI.

## 2. Methods and Materials

### 2.1 Reagents

Recombinant Murine IP-10/CXCL10 (P6740) was purchased from Beyotime Biotechnology Inc. (Shanghai, China). Recombinant neuregulin-1 $\beta$  (Nrg1, CYT-1186) was obtained from Prospec-Tany Technogene Ltd. (Ness-Ziona, Israel).

### 2.2 Animals and Cell Lines

Female C57BL/6 mice (three months old, from Guangdong Medical Laboratory Animal Center, Guangzhou, China) were housed at the Animal Center of Shantou University Medical College (SUMC) under specific pathogen-free conditions (25 °C, 12 h day/night controlled light cycle) and provided with food and water *ad libitum*. Animal experimental protocols followed the rules and regulations of the Ethics Committee of SUMC (SUMC2014-004) and conformed to the guidelines of the Chinese Animal Welfare Agency. HT22 and NSC34 mouse neuronal cells were purchased from Guangzhou Jennio Biotech Co., Ltd. (Guangzhou, China) and grown in dulbecco's modified eagle medium (DMEM) containing 10% fetal bovine serum. Both cell lines were authenticated at Jennio Biotech Co., Ltd. by short tandem repeat (STR) profiling. No contamination of mycoplasma has been identified by the company. HT22 cells and NSC34 cells are both neural cell lines. NSC34 cells are obtained from mouse spinal cord neural cells and HT22 cells are mouse hippocampal neurons. They are both used as excellent *in vitro* models for research of neuronal damage. Some studies use NSC34 cells as *in vitro* models for SCI while others use HT22 cells [17–20]. Therefore, in this study both cell lines were employed as *in vivo* models, which allows for a more comprehensive study of the effects of CXCL10 and Nrg1 on neurons.

### 2.3 GEO Data Analysis

Microarray datasets GSE42828 and GSE93561 were downloaded from Gene Expression Omnibus (GEO) and collected using the following platforms: GPL1261 [Mouse430\_2] Affymetrix Mouse Genome 430 2.0 Array. Gene expression matrices from two datasets were merged, inter-batch differences were removed, and the R package “ggplot2” was used for data visualization.

### 2.4 Mouse SCI

Mice were injected intraperitoneally with a mixture of xylazine (5 mg/kg, Sigma-Aldrich, Taufkirchen, Germany)

and ketamine (100 mg/kg, Fujian Gutian Pharmaceutical, Gutian, Fujian, China). A laminectomy was then performed at the T9-T11 levels. In the sham group mice, the spinal segment was exposed without damaging the dura, while in the SCI group mice the spinal cord was compressed for five seconds using a pair of forceps (RWD Life Science Co., Ltd., Shenzhen, China). Bladders were manually expressed once daily until a bladder reflex was established. Eight weeks post injury, three mice in each group were used for morphological assay and perfused with 4% paraformaldehyde solution (BL539A, Biosharp, Hefei, Anhui, China). After treatment with a 30% sucrose solution, spinal cord tissues were cryosectioned at 8  $\mu$ m thickness prior to further experiment.

### 2.5 Immunohistochemical Staining

Standard immunocytochemistry was performed as described previously [21]. Sections were rehydrated through a graded series of ethanol into phosphate buffer saline (PBS) and then subjected to heat-mediated antigen retrieval in sodium citrate antigen retrieval solution (C1010, Solarbio, Beijing, China) at 99 °C for 40 min. Sections were then blocked in 3% H<sub>2</sub>O<sub>2</sub> to clear endogenous peroxidase and incubated overnight at 4 °C with primary antibodies: rabbit anti-GFAP antibody (sc-33673, Santa Cruz Biotechnology, Dallas, TX, USA; 1:200), mouse anti-CD68 antibody (sc-20060, Santa Cruz, Dallas, TX, USA; 1:100), and rabbit anti-CXCL10 antibody (10937-1-AP, ProteinTech, Rosemont, IL, USA; 1:200). After washing three times in PBS for 10 min, sections were incubated with biotinylated secondary antibody and streptavidin-peroxidase conjugate at room temperature for 2 h. The AEC kit (Zhongshan Goldbridge Biotechnology Co., LTD., Zhongshan, Guangdong, China) was used to visualize antigen-antibody complexes. The stained sections were imaged using a Jiangnan light microscope (DN-10B, Jiangnan, Nanjing, Jiangsu, China). Quantification of the staining intensity was performed by densitometry using Image J software (V1.6, National Institutes of Health, Bethesda, MD, USA).

### 2.6 Immunofluorescent Staining

The spinal cord section pretreatment was described above in the section “Immunohistochemical staining”. Following incubation with antibody dilution buffer (Cat no. A1800, Solarbio, Beijing, China), sections were treated with a mixture of the primary rabbit anti-mouse CXCL10 antibody (10937-1-AP, ProteinTech, Rosemont, IL, USA; 1:200) and mouse anti-mouse  $\beta$ III-Tubulin antibody (sc-80005; Santa Cruz, Dallas, TX, USA; 1:200) [22]. Counterstaining was performed using 4',6-diamidino-2-phenylindole (DAPI; Beyotime Biotechnology, Shanghai, China). Fluorescence microscopy was performed using an Axio Imager Z2 fluorescence microscope (objective: 40 $\times$ /0.95; Carl Zeiss LSM880, Zeiss, Jena, Germany).

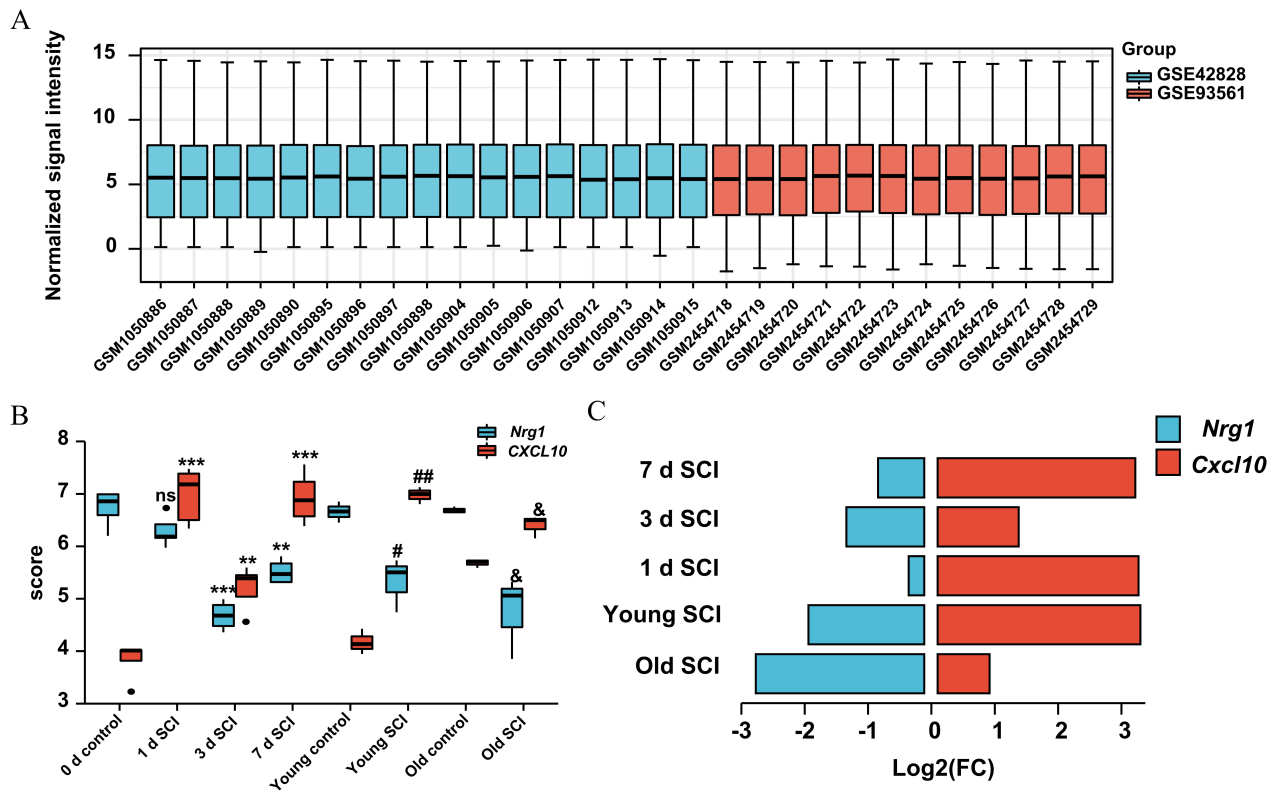


**Fig. 1. Expression of *Cxcl10* and *Nrg1* genes in microarray datasets GSE42828 and GSE93561.** (A) Gene expression matrices were merged with no inter-batch differences. (B) Expression score of *Cxcl10* and *Nrg1* genes in microarray datasets GSE42828 and GSE93561 (\*\*, vs. 0 d control,  $p < 0.01$ ; \*\*\*, vs. 0 d control,  $p < 0.001$ ; ###, vs. young control,  $p < 0.01$ ; #, vs. young control,  $p < 0.05$ ; &, vs. old control,  $p < 0.05$ ; ns, no significance). (C) Log<sub>2</sub> values in both *Cxcl10* and *Nrg1* expressions. Log<sub>2</sub> value indicates the quotient of expression quantity in the SCI group and that in the sham group taking the logarithm base 2. *Nrg1*, Neuregulin 1; *CXCL10*, C–X–C motif chemokine ligand 10; SCI, spinal cord injury.

### 2.7 Cell Viability Assay

Cell viability was determined using a CCK-8 assay (C0041, Beyotime Biotechnology, Shanghai, China). HT22 and NSC34 cells were seeded into 96-well plates ( $1 \times 10^3$  cells/well) for 12 h. After treatment with CXCL10 (0–10 nM) or Nrg1 (0–10 nM) as well as a mixture of CXCL10 (5 nM) and Nrg1 (5 nM) for 12 h, HT22 and NSC34 mouse neuronal cells were treated with fresh DMEM containing 10% CCK-8. Absorbance was then measured using a microplate reader (Bio-Tek, Winooski, VT, USA). Cell viability was expressed as the percentage of vehicle control absorbance at 450 nm.

### 2.8 HT22 Cells and NSC34 Cells Scratch Injury Model

Cells were seeded in a 12-well plate at a concentration of  $2 \times 10^5$  cells/well. When confluence reached 80%, cultured cells were scratched across the cell surface vertically by a 200  $\mu$ L pipette tip and unattached cells were washed away by fresh DMEM. 1 mL DMEM with CXCL10 (5 nM), Nrg1 (5 nM), or a mixture of CXCL10 (5 nM) and Nrg1 (5 nM) were then individually added. Cells in the control group were treated with DMEM. The scratch area

and wound coverage of the total area were determined at 0, 6, 12, 24 and 48 hours post injury. The percentage of wound closure was calculated using the following formula, in which  $A_{t=0}$  is the initial wound area, and  $A_{t=\Delta t}$  is the wound area after  $\Delta t$  hours of the initial scratch [23].

$$\% \text{ of Wound Closure} = \left( \frac{A_{t=0} - A_{t=\Delta t}}{A_{t=0}} \right) \times 100\% \quad (1)$$

### 2.9 Western Blot Analysis

HT22 and NSC34 cells were lysed in RIPA lysis buffer (P0013B, Beyotime Biotechnology, Shanghai, China) with Phenylmethanesulfonyl fluoride (PMSF, ST506, Beyotime Biotechnology, Shanghai, China) and Phosphatase inhibitor (PPI, P1081, Beyotime Biotechnology, Shanghai, China) to prepare protein samples. Proteins were separated by SDS–polyacrylamide gel electrophoresis and transferred to polyvinylidene difluoride membranes (0.45  $\mu$ m; Merck Millipore Ltd., Darmstadt, Germany). After blocking for one hour with 5% bovine serum albumin, membranes were incubated with the appropriate primary (Anti-phosphor-ErbB4 antibody (bs-3220R, Bioss, Bei-

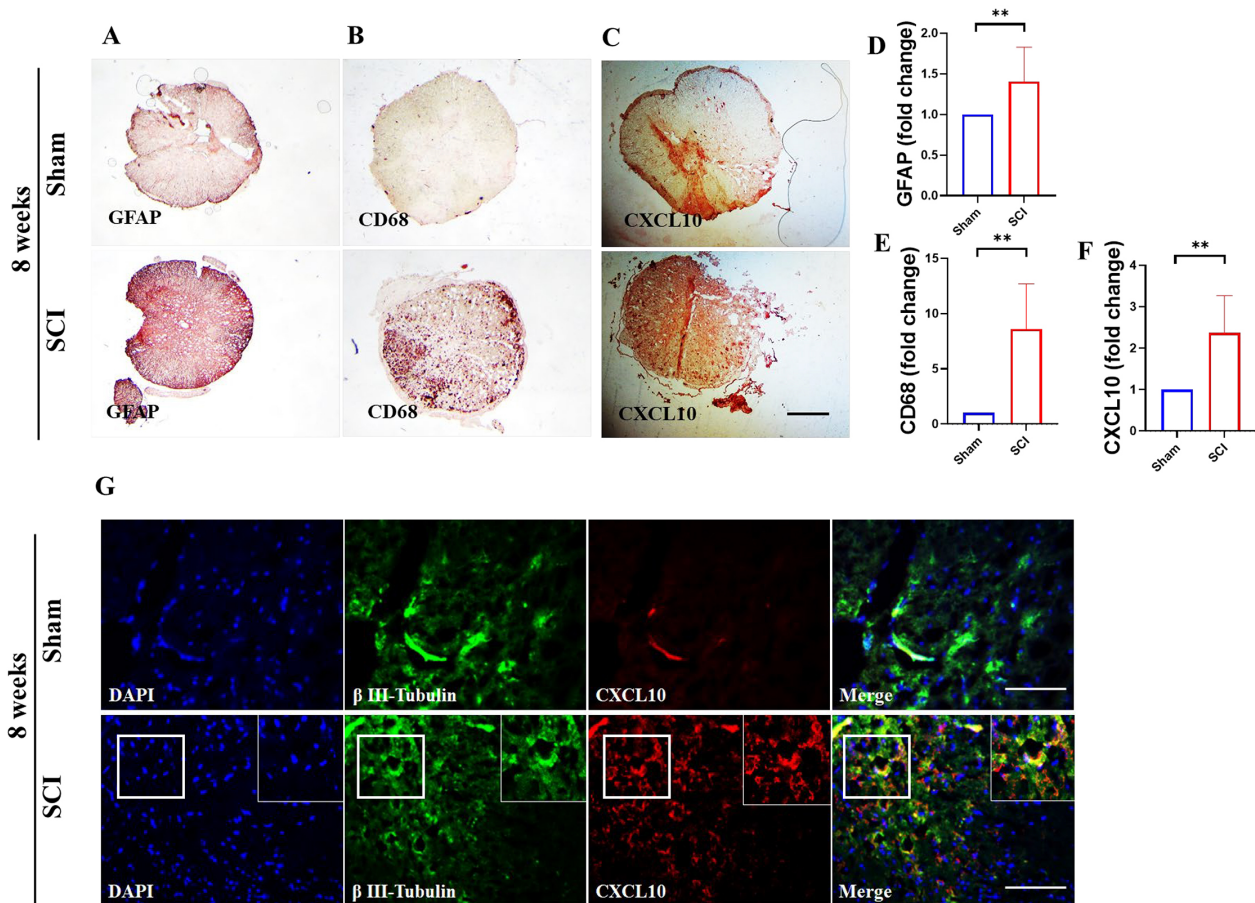


**Fig. 2. SCI of mice causes inflammation in the spinal cord.** (A–F) In SCI mice, high expression levels of GFAP (A,D), CD68 (B,E), and CXCL10 (C,F) were observed in the injured spinal cord. Scar bar: 200  $\mu$ m. S.E.M. (\*\* $p < 0.01$ ). (G) Representative immunofluorescence image of the spinal cord of mice eight weeks after SCI staining with  $\beta$ III-Tubulin and CXCL10 is shown. Scar bar: 50  $\mu$ m. GFAP, Glial Fibrillary Acidic Protein; CXCL10, C–X–C motif chemokine ligand 10; DAPI, 4',6-diamidino-2-phenylindole.

jing, China), anti-ErbB4 antibody (sc-71071, Santa Cruz, Dallas, TX, USA), anti-phosphor-ERK1/2 antibody (sc-136521, Santa Cruz, Dallas, TX, USA), anti-ERK1/2 antibody (sc-514302, Santa Cruz, Dallas, TX, USA), anti-caspase 9 antibody (AF1264, Beyotime Biotechnology, Shanghai, China), anti-caspase 3 antibody (P17, Boster, Wuhan, Hubei, China) and anti-GAPDH antibody (sc-365062, Santa Cruz, Dallas, TX, USA), and secondary antibodies. The protein bands were quantified using a gel imaging analysis system (Tanon-2500B, Tanon, Shanghai, China). The signal intensity was quantified by densitometry using Image J software (V1.6, National Institutes of Health, Bethesda, MD, USA).

### 2.10 Statistical Analysis

Statistical testing was implemented using Statistical Package for the Social Sciences software (SPSS, Version 20.0, Chicago, IL, USA). Differences between two groups were compared by Student's *t*-test. The data were given as the mean  $\pm$  standard error of the mean (SEM). The *p*-values are given in the Figure legends.

## 3. Results

### 3.1 Expression of CXCL10 and Nrg1 in SCI Mice

Microarray dataset profiles GSE42828 and GSE93561 were downloaded from GEO DataSets. After normalization, probes were converted to gene symbols for series matrix files of each dataset and the gene expression data of these two datasets were merged (Fig. 1A). The differential expressions of *Cxcl10* and *Nrg1* genes in both datasets were tested and it was found that the expression level of *Cxcl10* is significantly up-regulated in SCI samples, whereas that of *Nrg1* is significantly down-regulated in the three-day and seven-day SCI groups, the young SCI group, and the old SCI group when compared with control samples (Fig. 1B).

After  $\log_2$  transformation, it was also found that in SCI mice of different ages or at different time points post SCI, the *Cxcl10* and *Nrg1* genes showed different expression quantities (Fig. 1C). The  $\log_2$  value gives the quotient of expression quantity in the SCI group and the sham group after taking the base 2 logarithm.  $\log_2$  values in both the *Cxcl10* and *Nrg1* gene expressions of the young group were higher than those of the old group.  $\log_2$  value analysis

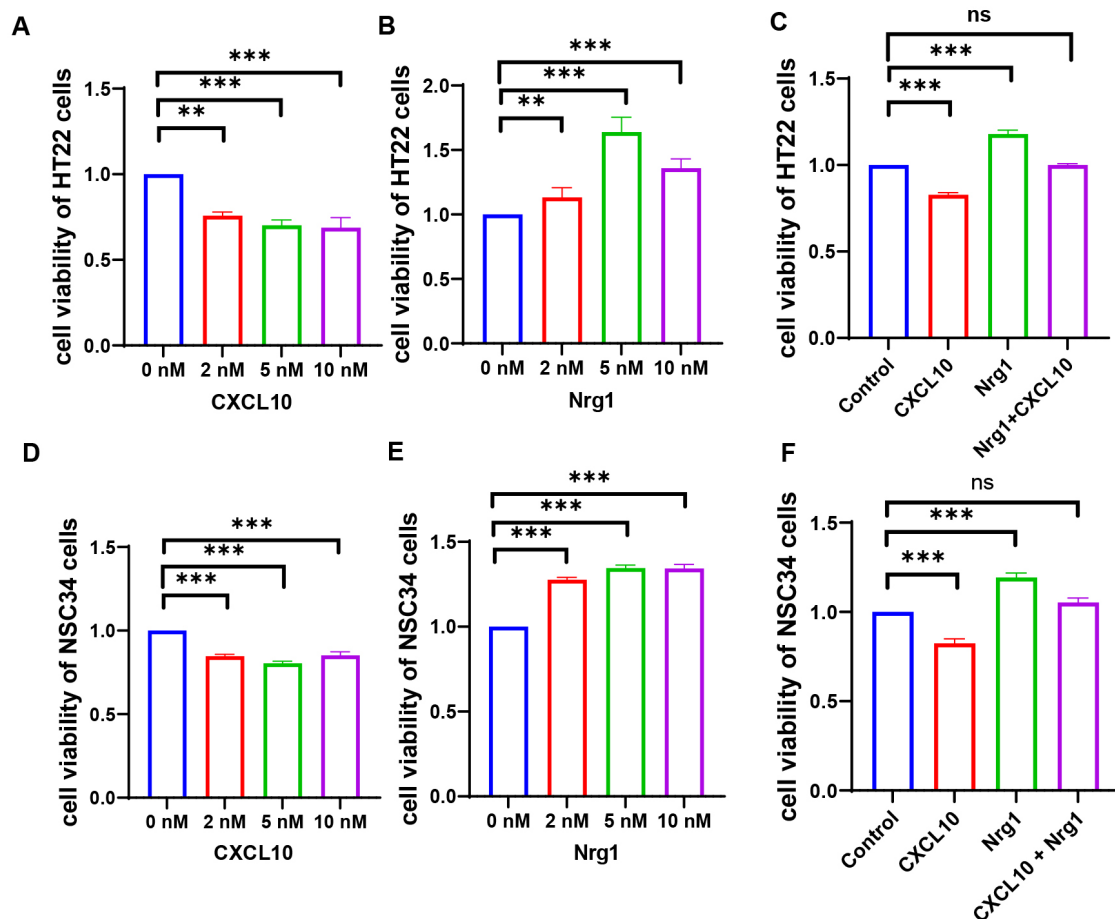


**Fig. 3. Effect of CXCL10 and Nrg1 on HT22 cells or NSC34 cells viability.** (A–C) Effect of CXCL10 (A) and Nrg1 (B), as well as combined effects of the two (C) on HT22 cell viability.  $n = 10$  per group. S.E.M. (\*\*\*,  $p < 0.001$ ; \*\*,  $p < 0.01$ ; ns, no significance). (D–F) Effect of CXCL10 (D) and Nrg1 (E), as well as combined effects of the two (F) on NSC34 cell viability.  $n = 10$  per group. S.E.M. (\*\*\*,  $p < 0.001$ ; ns, no significance). Nrg1, Neuregulin 1.

demonstrated that compared to the vehicle control, *Nrg1* expression is reduced at three and seven days post injury. It was also noted there was a minimum  $\log_2$  value of *Cxcl10* at three days post injury. That means that *Cxcl10* expression is increased post injury, but moderated at three days post injury.

It was next aimed at determining whether CXCL10 is involved in neuronal injury. To address this, mouse spinal cord slices were harvested for immunohistochemical and immunofluorescence staining at eight weeks following SCI or sham operation. By using immunohistochemical staining, it was demonstrated that CD68, GFAP, and CXCL10 levels were significantly increased eight weeks post injury when compared with sham controls. These data suggest that SCI causes glial cell activation, accompanied by enhanced expression of CXCL10 (Fig. 2A–F).

Additionally, immunofluorescence staining showed partial localization of CXCL10 adjacent to  $\beta$ III-Tubulin-positive neuronal fibers, suggesting a direct impact of CXCL10 on neurons under the pathological conditions of SCI (Fig. 2G).

### 3.2 Effect of CXCL10 and Nrg1 on HT22 and NSC34 Cells Viability

To determine whether CXCL10 intensifies neuronal cell damage, the viability of HT22 and NSC34 cells was initially assessed. A similar phenomenon occurred when HT22 and NSC34 cells were treated for 12 h with a serial concentration of CXCL10 (0–10 nM). It appears that 2, 5 and 10 nM of CXCL10 reduced cell viability in both cell types (Fig. 3A,D). Both cell types were then treated with Nrg1 (0–10 nM) for 12 h, to explore the basic effect of Nrg1. Nrg1 increased cell viability in a dose-dependent manner at doses ranging from 2 to 5 nM (Fig. 3B,E). Nrg1 and CXCL10 were both then assessed, either individually or in combination, at 5 nM to evaluate how the two cooperated in HT22 and NSC34 cells (Fig. 3C,F). The CCK8 assay results showed that the CXCL10-induced decrease in cell viability was significantly rescued by Nrg1.

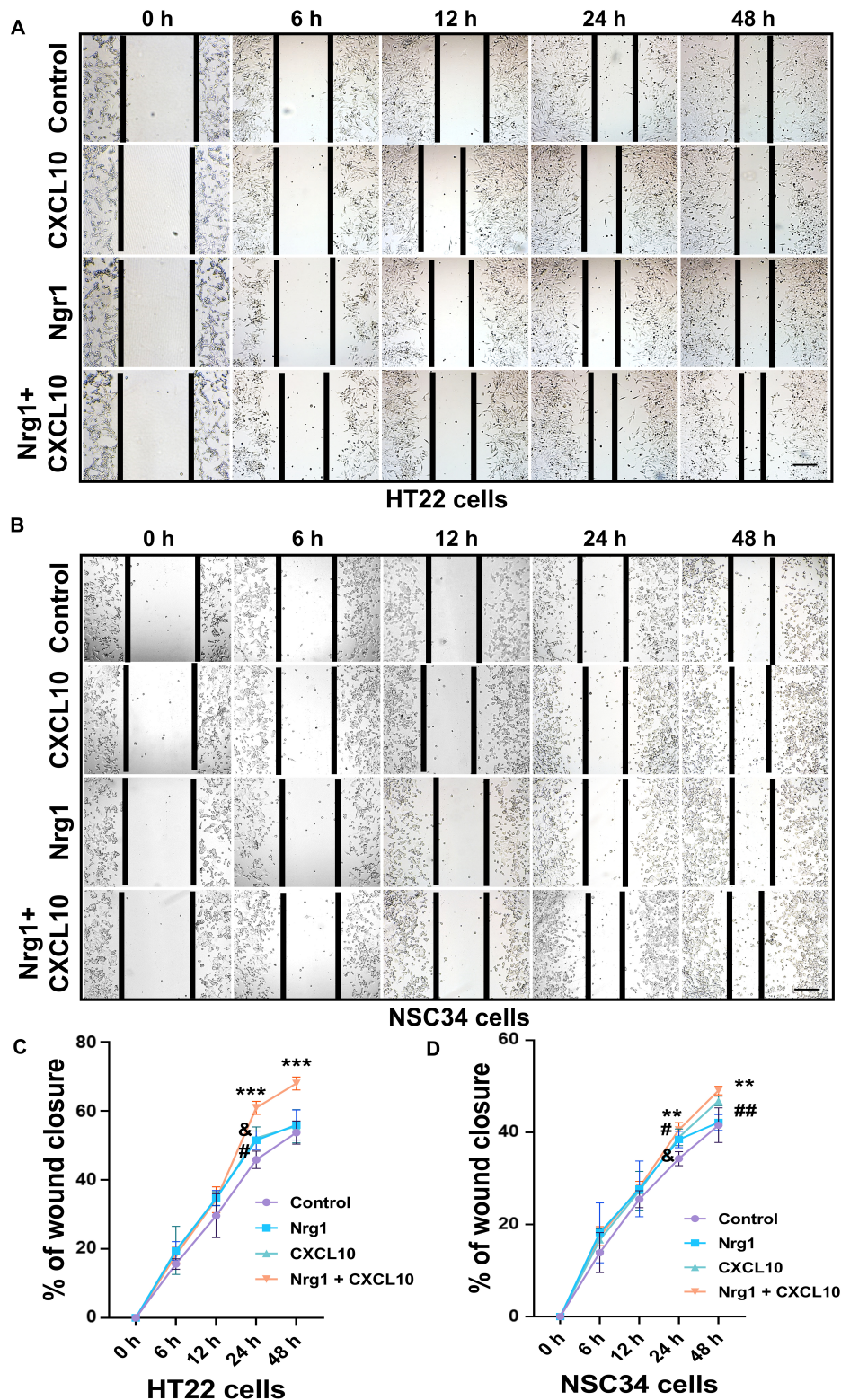


**Fig. 4. Effect of CXCL10 and Nrg1 on HT22 cells and NSC34 cells after scratch injury.** (A,C) Effect of CXCL10 and Nrg1 on HT22 cells after scratch injury.  $n = 4$  per group. Scar bar: 200  $\mu\text{m}$ . S.E.M. (\*\*\*, Nrg1 + CXCL10 group vs. control group,  $p < 0.001$ ; #, CXCL10 group vs. control group,  $p < 0.05$ ; &, Nrg1 group vs. control group,  $p < 0.05$ ). (B,D) Effect of CXCL10 and Nrg1 on NSC34 cells after scratch injury.  $n = 4$  per group. Scar bar: 200  $\mu\text{m}$ . S.E.M. (\*\*, Nrg1 + CXCL10 group vs. control group,  $p < 0.001$ ; ##, CXCL10 group vs. control group,  $p < 0.01$ ; #, CXCL10 group vs. control group,  $p < 0.05$ ; &, Nrg1 group vs. control group,  $p < 0.05$ ).

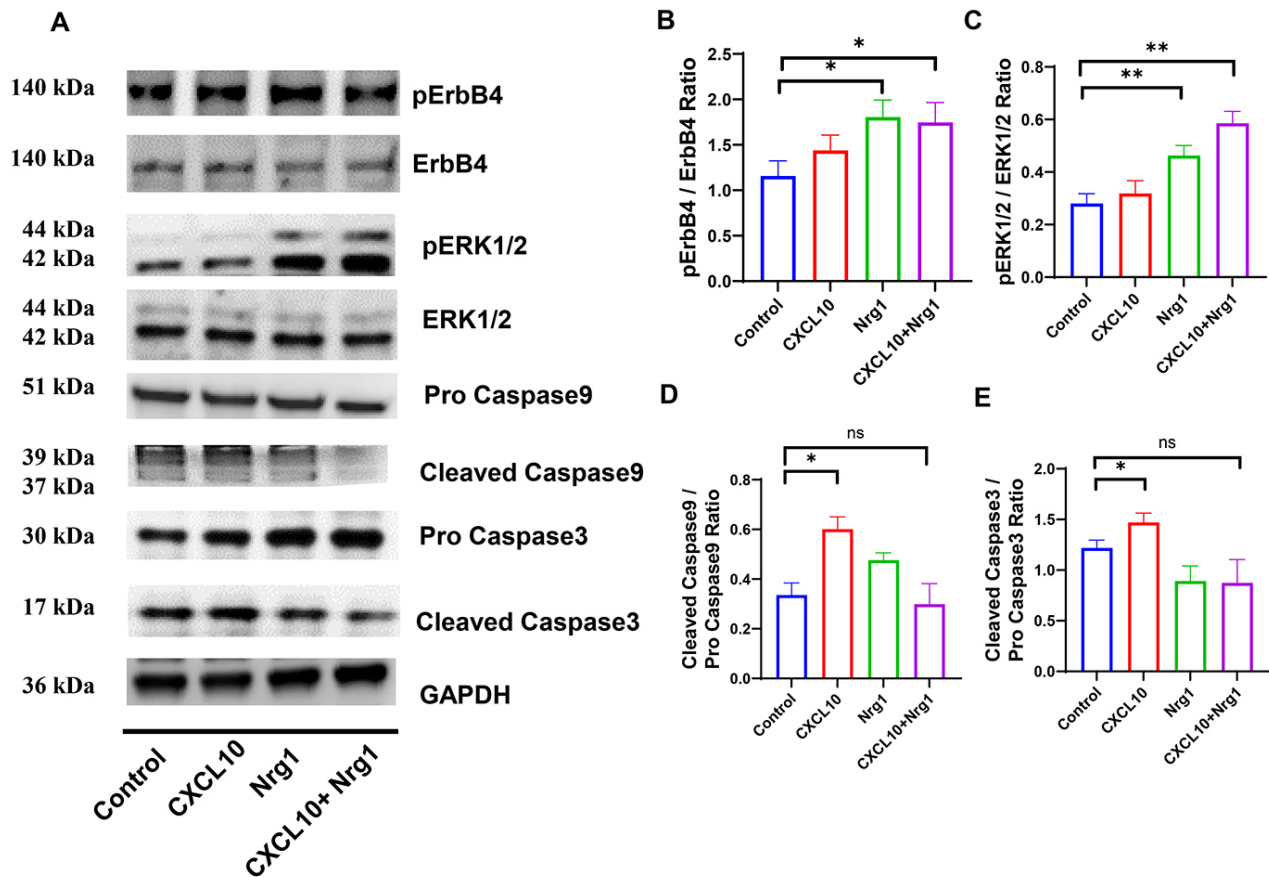


**Fig. 5. Effect of CXCL10 and Nrg1 on the molecular expression of HT22 cells.** (A) Representative images of pErbB4, pERK1/2, cleaved caspase 9, and cleaved caspase 3. (B–E) Quantitative results of pErbB4, pERK1/2, cleaved caspase 9, and cleaved caspase 3.  $n = 3$  per group. S.E.M. (\*\* $p < 0.01$ ; \* $p < 0.05$ ; ns, no significance). GAPDH, glyceraldehyde-3-phosphate dehydrogenase.

### 3.3 Effect of CXCL10 and Nrg1 on Scratch-Induced Wound Healing of HT22 and NSC34 Cells

Scratch-injury assay was used to clarify the role of CXCL10 and Nrg1 in recovery from neuronal injury. Scratch injury activated the primary damage of neurons and then affected the entire neuronal migration, which to a certain degree mimics neuronal injury under the pathological condition of SCI. Therefore, it is appropriate to monitor the neuronal response after SCI *in vitro* with the use of the scratch assay [19]. In both HT22 and NSC34 cells, microscopic imaging revealed that wound closure failed to be inhibited in the CXCL10 group. Intriguingly, CXCL10 promoted scratch healing in HT22 cells at 24 h, and in NSC34 cells at 24 and 48 h (Fig. 4A–D). Wound closure was significantly increased by Nrg1 at 24 h after scratch in both cell types (Fig. 4A–D). Nrg1 and CXCL10 co-treated HT22 and NSC34 cells showed significant wound closure 24 and 48 h following scratch injury (Fig. 4A–D).

### 3.4 Effect of CXCL10 and Nrg1 on Related Molecules in HT22 and NSC34 Cells

Next, we wanted to investigate the effects of CXCL10 and NRG1 on related molecules in HT22 and NSC34 cells.

The protein levels of pErbB4, pERK1/2, cleaved caspase 9, and cleaved caspase 3 were detected in HT22 and NSC34 cells (Fig. 5A and Fig. 6A). Nrg1 binds to ErbB4 and promotes its phosphorylation [24]. Cleaved caspase 9 and cleaved caspase 3 play an apoptosis-promoting role [11]. pERK1/2 is involved in cell migration, cell survival and cell proliferation [25,26]. These molecules may serve as downstream molecules of CXCL10 or Nrg1 to perform critical functions.

In HT22 cells results showed that, compared with the sham group, CXCL10 induced an increase in the expressions of cleaved caspase 9 and cleaved caspase 3, with no distinct difference in the level of pERK1/2 (Fig. 5D,E). High levels of cleaved caspase 9, cleaved caspase 3, and pERK1/2 were observed in CXCL10-treated NSC34 cells (Fig. 6D,E), although Nrg1 treatment induced an increase in the level of pErbB4 and pERK1/2 in both cell lines (Fig. 5B–D and Fig. 6B–D). Additionally, Nrg1 mitigated the expressions of cleaved caspase 9 and cleaved caspase 3 induced by CXCL10, accompanied by enhanced phosphorylation levels of ERK1/2 in both cell lines (Fig. 5D,E and Fig. 6D,E).

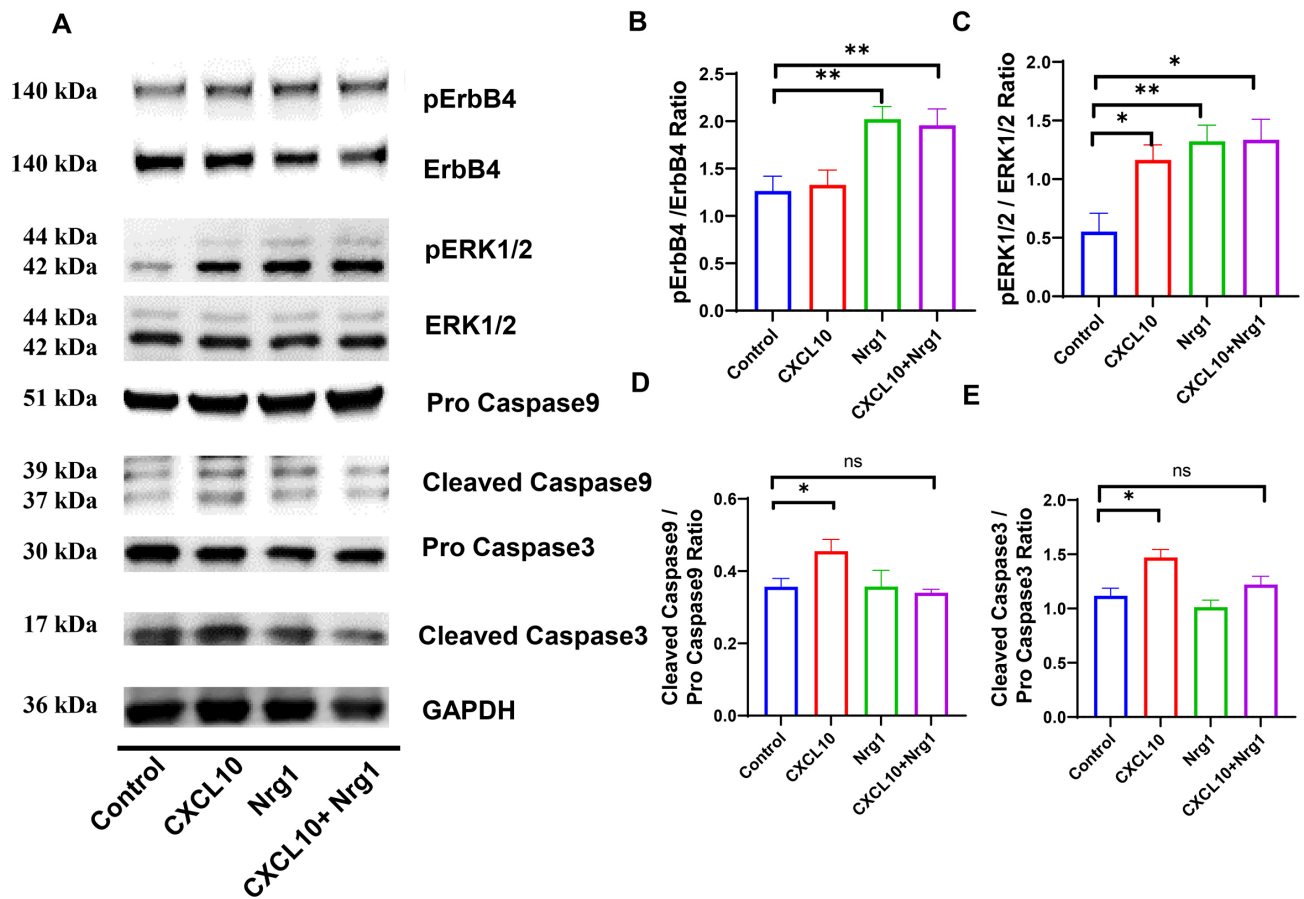


**Fig. 6. Effect of CXCL10 and Nrg1 on the molecular expression of NSC34 cells.** (A) Representative images of pErbB4, pERK1/2, cleaved caspase 9, and cleaved caspase 3. (B–E) Quantitative results of pErbB4, pERK1/2, cleaved caspase 9, and cleaved caspase 3.  $n = 3$  per group. S.E.M. (\*\* $p < 0.01$ ; \* $p < 0.05$ ; ns, no significance).

#### 4. Discussion

In this study, the expression levels of *Cxcl10* and *Nrg1* genes were identified as GSE42828 and GSE93561 from GEO DataSets. Notably, it was found that *Cxcl10* expression significantly increased during both acute and subacute (0–7 d) SCI in mice, as well as in both young and old mice, suggesting that enhanced *Cxcl10* expression is a common characteristic of SCI. SCI mice were then analyzed eight weeks post-injury. It was shown that the level of CXCL10 remained high even at eight weeks post-SCI. The fluorescent images of the injured spinal cord demonstrated partial adjacent localization of CXCL10 and  $\beta$ III-tubulin, indicating that CXCL10 may exert a direct impact on neurons. The pathological effect of CXCL10 on HT22 and NSC34 cells was further tested. Additionally, the potential influence of Nrg1 on these effects was also analyzed. CXCL10 induced a decrease in cell viability, partially reversed by Nrg1.

Despite its negative effect on cell viability, CXCL10 failed to inhibit the scratch healing of HT22 and NSC34 cells. This suggests that CXCL10 is involved in scratch healing with complicated actions. In the cell scratch assay, there are two options for scratch healing: one is that cells spontaneously migrate from the edge of the scratch

area into the gap and the other is that cells are squeezed by other cells and then extended to the gap. CXCL10 attracts and promotes the infiltration of immune cells and the migration of cancer cells. M2 macrophages, CD8<sup>+</sup> T cells, and NK cells are observed to migrate toward CXCL10 [27–30]. In carcinogenic diseases, CXCL10 promotes the migration of prostate, breast, leukemic, and pancreatic cancer cells [31,32]. Therefore, it is hypothesized here that the migration promotion effect of CXCL10 may partially counteract its apoptosis-promoting effect, leading to no inhibitory effect of scratch wound healing. It was also observed that the co-treatment of Nrg1 and CXCL10 had better therapeutic effect on scratch healing than a single treatment using either Nrg1 or CXCL10. This indicated that Nrg1 might partly antagonize the apoptotic effect of CXCL10.

Ongoing evidence has shown a variety of roles for Nrg1 in the regulation of central nervous system injury and repair processes. Nrg1 positively regulates nerve cell-like neural crest cells (NCCs) and neural precursor cells (NPCs). NCCs, expressing ErbB2 and ErbB4 receptors, respond to paracrine effects of Nrg1 during development [33]. Nrg1 also regulates pathfinding and migration of NCCs [34]. NPCs from the E14 mouse striatum germinal zone express

Nrg1 and Nrg1 and regulate the proliferation of NPCs *in vitro* [35]. In the rat SCI model, Nrg1 $\beta$ 1 has been shown to provide neuroprotection through alleviating reactive oxygen species and apoptosis [36]. In this study, Nrg1 also promoted scratch healing by improving cell growth in both HT22 and NSC34 cells, further confirming the feasibility of NRG1 therapy in SCI.

Finally, the effects of CXCL10 and Nrg1 on HT22 and NSC34 cells were analyzed at the molecular level. Sui *et al.* [11,37] reported that CXCL10 induces apoptosis via the activation of caspase 3 and caspase 9. According to Chen *et al.* [26], Nrg1 promotes cell survival through the pERK pathway. CXCL10 also induces macrophage migrations with the activation of the ERK1/2 signaling pathway [38]. In concordance with previous studies, the results reported here show that CXCL10-activated cleaved caspase 3 and cleaved caspase 9 were inhibited by Nrg1, indicating that Nrg1 inhibits CXCL10-mediated neuronal apoptosis by inhibiting its apoptosis-promoting effect via the ERK signaling pathway. It was also found that the ERK1/2 signaling pathway played a critical role in many aspects of this study. ERK1/2 activation functions not only as the downstream effector of Nrg1/pErbB4 signaling pathway involved in cell survival, but also in cell migration promotion in NSC34 cells.

## 5. Conclusions

In summary, CXCL10 shows an up-regulated expression and Nrg1 shows a down-regulated expression during SCI. Additionally, the present study indicates that neutralization of CXCL10 reduces cell apoptosis [10,39]. When comparing these results to those in previously reported studies, it can be concluded that CXCL10 results in apoptosis of HT22 and NSC34 cells rather than inhibition of wound closure *in vitro*. Nrg1 may protect neurons by partly antagonizing the effect of CXCL10. Further research is needed to identify neuronal loss aggravation by CXCL10 via the enhancement of inflammatory response.

## Availability of Data and Materials

The microarray datasets analyzed during the current study are available from <https://www.ncbi.nlm.nih.gov/gco>. Other data generated or analyzed during this study are included in this published article.

## Author Contributions

WJZ, XYQ, CC and YQS designed the research study. XYQ, WZ, QL, CL and JJD performed the research. CC and YQS provided help and advice on establishing the mouse spinal cord injury model. XYQ, CMQ and YW analyzed the data. XYQ, WJZ and YW wrote the manuscript. All authors contributed to editorial changes in the manuscript. All authors read and approved the final manuscript. All authors have participated sufficiently

in the work and agreed to be accountable for all aspects of the work.

## Ethics Approval and Consent to Participate

The animal experimental followed the rules and regulations of the Ethics Committee of Shantou University Medical College. Ethical approval number: SUMC2014-004.

## Acknowledgment

We thank anonymous reviewers whose constructive comments and suggestions would help improve the quality of our manuscript.

## Funding

The authors acknowledge funding sources from the National Natural Science Foundation of China (Grant No. 81471279 and 81171138). Jiangsu Province Shuangchuang Talent Plan (Grant No. JSSCRC 2021533), the Research Start-up Fund of Jiangnan University (Grant No. 1285081903200020), and the Research Start-up Fund of Wuxi School of Medicine, Jiangnan University (Grant No. 1286010242190060).

## Conflict of Interest

The authors declare no conflict of interest.

## References

- [1] Kumar R, Lim J, Mekary RA, Rattani A, Dewan MC, Sharif SY, *et al.* Traumatic Spinal Injury: Global Epidemiology and Worldwide Volume. *World Neurosurgery*. 2018; 113: e345–e363.
- [2] Fan B, Wei Z, Feng S. Progression in translational research on spinal cord injury based on microenvironment imbalance. *Bone Research*. 2022; 10: 35.
- [3] Alexander JK, Popovich PG. Neuroinflammation in spinal cord injury: therapeutic targets for neuroprotection and regeneration. *Progress in Brain Research*. 2009; 175: 125–137.
- [4] Donnelly DJ, Popovich PG. Inflammation and its role in neuroprotection, axonal regeneration and functional recovery after spinal cord injury. *Experimental Neurology*. 2008; 209: 378–388.
- [5] Jones TB, McDaniel EE, Popovich PG. Inflammatory-mediated injury and repair in the traumatically injured spinal cord. *Current Pharmaceutical Design*. 2005; 11: 1223–1236.
- [6] Trivedi A, Olivas AD, Noble-Haesslein LJ. Inflammation and Spinal Cord Injury: Infiltrating Leukocytes as Determinants of Injury and Repair Processes. *Clinical Neuroscience Research*. 2006; 6: 283–292.
- [7] Knerlich-Lukoschus F, Held-Feindt J. Chemokine-ligands/receptors: multiplayers in traumatic spinal cord injury. *Mediators of Inflammation*. 2015; 2015: 486758.
- [8] McTigue DM, Tani M, Krivacic K, Chemosky A, Kelner GS, Maciejewski D, *et al.* Selective chemokine mRNA accumulation in the rat spinal cord after contusion injury. *Journal of Neuroscience Research*. 1998; 53: 368–376.
- [9] Rice T, Larsen J, Rivest S, Yong VW. Characterization of the early neuroinflammation after spinal cord injury in mice. *Journal of Neuropathology and Experimental Neurology*. 2007; 66: 184–195.
- [10] Gonzalez R, Hickey MJ, Espinosa JM, Nistor G, Lane TE,

- Keirstead HS. Therapeutic neutralization of CXCL10 decreases secondary degeneration and functional deficit after spinal cord injury in mice. *Regenerative Medicine*. 2007; 2: 771–783.
- [11] Sui Y, Stehno-Bittel L, Li S, Loganathan R, Dhillon NK, Pinson D, *et al.* CXCL10-induced cell death in neurons: role of calcium dysregulation. *The European Journal of Neuroscience*. 2006; 23: 957–964.
- [12] Kataria H, Alizadeh A, Karimi-Abdolrezaee S. Neuregulin-1/ErbB network: An emerging modulator of nervous system injury and repair. *Progress in Neurobiology*. 2019; 180: 101643.
- [13] Bartus K, Galino J, James ND, Hernandez-Miranda LR, Dawes JM, Fricker FR, *et al.* Neuregulin-1 controls an endogenous repair mechanism after spinal cord injury. *Brain*. 2016; 139: 1394–1416.
- [14] Ding Z, Dai C, Zhong L, Liu R, Gao W, Zhang H, *et al.* Neuregulin-1 converts reactive astrocytes toward oligodendrocyte lineage cells via upregulating the PI3K-AKT-mTOR pathway to repair spinal cord injury. *Biomedicine & Pharmacotherapy*. 2021; 134: 111168.
- [15] Xiang W, Jiang L, Zhou Y, Li Z, Zhao Q, Wu T, *et al.* The lncRNA Ftx/miR-382-5p/Nrg1 axis improves the inflammation response of microglia and spinal cord injury repair. *Neurochemistry International*. 2021; 143: 104929.
- [16] Harbuzariu A, Pitts S, Cespedes JC, Harp KO, Nti A, Shaw AP, *et al.* Modelling heme-mediated brain injury associated with cerebral malaria in human brain cortical organoids. *Scientific Reports*. 2019; 9: 19162.
- [17] Wang N, Yu H, Song Q, Mao P, Li K, Bao G. Sesamol-loaded stearic acid-chitosan nanomicelles mitigate the oxidative stress-stimulated apoptosis and induction of pro-inflammatory cytokines in motor neuronal of the spinal cord through NF- $\kappa$ B signaling pathway. *International Journal of Biological Macromolecules*. 2021; 186: 23–32.
- [18] Kim W, Cho SB, Jung HY, Yoo DY, Oh JK, Choi GM, *et al.* Phosphatidylethanolamine-Binding Protein 1 Ameliorates Ischemia-Induced Inflammation and Neuronal Damage in the Rabbit Spinal Cord. *Cells*. 2019; 8: 1370.
- [19] Valeri A, Chiricosta L, Gugliandolo A, Pollastro F, Mazzon E. Will Cannabigerol Trigger Neuroregeneration after a Spinal Cord Injury? An *In Vitro* Answer from NSC-34 Scratch-Injured Cells Transcriptome. *Pharmaceuticals*. 2022; 15: 117.
- [20] Zhang L, Han P. Neural stem cell-derived exosomes suppress neuronal cell apoptosis by activating autophagy via miR-374-5p/STK-4 axis in spinal cord injury. *Journal of Musculoskeletal & Neuronal Interactions*. 2022; 22: 411–421.
- [21] Yang Z, Jiang Q, Chen SX, Hu CL, Shen HF, Huang PZ, *et al.* Differential changes in Neuregulin-1 signaling in major brain regions in a lipopolysaccharide-induced neuroinflammation mouse model. *Molecular Medicine Reports*. 2016; 14: 790–796.
- [22] Chen L, Gao X, Zhao S, Hu W, Chen J. The Small-Molecule TrkB Agonist 7, 8-Dihydroxyflavone Decreases Hippocampal Newborn Neuron Death After Traumatic Brain Injury. *Journal of Neuropathology and Experimental Neurology*. 2015; 74: 557–567.
- [23] Li D, Huang S, Zhu J, Hu T, Han Z, Zhang S, *et al.* Exosomes from MiR-21-5p-Increased Neurons Play a Role in Neuroprotection by Suppressing Rab11a-Mediated Neuronal Autophagy *In Vitro* After Traumatic Brain Injury. *Medical Science Monitor*. 2019; 25: 1871–1885.
- [24] Ou GY, Lin WW, Zhao WJ. Neuregulins in Neurodegenerative Diseases. *Frontiers in Aging Neuroscience*. 2021; 13: 662474.
- [25] Nozaki K, Nishimura M, Hashimoto N. Mitogen-activated protein kinases and cerebral ischemia. *Molecular Neurobiology*. 2001; 23: 1–19.
- [26] Chen S, Hou Y, Zhao Z, Luo Y, Lv S, Wang Q, *et al.* Neuregulin-1 Accelerates Functional Motor Recovery by Improving Motoneuron Survival After Brachial Plexus Root Avulsion in Mice. *Neuroscience*. 2019; 404: 510–518.
- [27] Vogel DYS, Heijnen PDAM, Breur M, de Vries HE, Tool ATJ, Amor S, *et al.* Macrophages migrate in an activation-dependent manner to chemokines involved in neuroinflammation. *Journal of Neuroinflammation*. 2014; 11: 23.
- [28] Schoenborn JR, Wilson CB. Regulation of interferon-gamma during innate and adaptive immune responses. *Advances in Immunology*. 2007; 96: 41–101.
- [29] Lindell DM, Lane TE, Lukacs NW. CXCL10/CXCR3-mediated responses promote immunity to respiratory syncytial virus infection by augmenting dendritic cell and CD8(+) T cell efficacy. *European Journal of Immunology*. 2008; 38: 2168–2179.
- [30] Sidahmed AME, León AJ, Bosinger SE, Banner D, Danesh A, Cameron MJ, *et al.* CXCL10 contributes to p38-mediated apoptosis in primary T lymphocytes *in vitro*. *Cytokine*. 2012; 59: 433–441.
- [31] Hirth M, Gandla J, Höper C, Gaida MM, Agarwal N, Simonetti M, *et al.* CXCL10 and CCL21 Promote Migration of Pancreatic Cancer Cells Toward Sensory Neurons and Neural Remodeling in Tumors in Mice, Associated With Pain in Patients. *Gastroenterology*. 2020; 159: 665–681.e13.
- [32] Alassaf E, Mueller A. The role of PKC in CXCL8 and CXCL10 directed prostate, breast and leukemic cancer cell migration. *European Journal of Pharmacology*. 2020; 886: 173453.
- [33] Britsch S, Li L, Kirchhoff S, Theuring F, Brinkmann V, Birchmeier C, *et al.* The ErbB2 and ErbB3 receptors and their ligand, neuregulin-1, are essential for development of the sympathetic nervous system. *Genes & Development*. 1998; 12: 1825–1836.
- [34] Golding JP, Trainor P, Krumlauf R, Gassmann M. Defects in pathfinding by cranial neural crest cells in mice lacking the neuregulin receptor ErbB4. *Nature Cell Biology*. 2000; 2: 103–109.
- [35] Calaoa V, Rogister B, Bismuth K, Murray K, Brandt H, Lepince P, *et al.* Neuregulin signaling regulates neural precursor growth and the generation of oligodendrocytes *in vitro*. *The Journal of Neuroscience*. 2001; 21: 4740–4751.
- [36] Shahsavani N, Alizadeh A, Kataria H, Karimi-Abdolrezaee S. Availability of neuregulin-1beta1 protects neurons in spinal cord injury and against glutamate toxicity through caspase dependent and independent mechanisms. *Experimental Neurology*. 2021; 345: 113817.
- [37] Sui Y, Potula R, Dhillon N, Pinson D, Li S, Nath A, *et al.* Neuronal apoptosis is mediated by CXCL10 overexpression in simian human immunodeficiency virus encephalitis. *The American Journal of Pathology*. 2004; 164: 1557–1566.
- [38] Hua X, Ge S, Zhang M, Mo F, Zhang L, Zhang J, *et al.* Pathogenic Roles of CXCL10 in Experimental Autoimmune Prostatitis by Modulating Macrophage Chemotaxis and Cytokine Secretion. *Frontiers in Immunology*. 2021; 12: 706027.
- [39] Glaser J, Gonzalez R, Sadr E, Keirstead HS. Neutralization of the chemokine CXCL10 reduces apoptosis and increases axon sprouting after spinal cord injury. *Journal of Neuroscience Research*. 2006; 84: 724–734.